PACS numbers: 82.20.Db, 82.20.Pm, 82.20.Xr, 82.30.Fi, 82.39.Jn

The Wavelet Method for the Analysis of Electron-Transfer Kinetics in Bacterial Reaction Centres

Yu. M. Barabash, M. A. Zabolotny*, and T. V. Serdenko

Institute of Physics, National Academy of Sciences of Ukraine,
46 Nauky Av.,
03028 Kyyiv, Ukraine
*Taras Shevchenko Kyyiv National University,
64 Volodymyrska Str.,
01033 Kyyiv, Ukraine

In a given paper, kinetics of electron transfer in bacterial reactive centres (RC) is discussed. Aspects of relaxation processes and photoinduced structural changes in a molecular complex RC of Rhodobacter sphaeroides as a result of intramolecular electron transfer are studied by the wavelet analysis. Relaxation kinetics has S-shaped character of the time-dependence of a constant of rate of electron return from an acceptor after turning off stimulating light. Relaxation curves of RC are non-stationary (time-dependent). Two-level model of electron transfer is considered. Reaction centres are regarded as dynamic in time and identical with each other. Wavelet analysis of relaxation kinetics allows us to assume that exponents of relaxation curves are not involved simultaneously, but appear by turns.

В данной работе обсуждается кинетика переноса электронов в бактериальных реактивных центрах (РЦ). Аспекты релаксационных процессов и фотоиндуцированных структурных изменений в молекулярном комплексе РЦ Rhodobacter sphaeroides как результат внутримолекулярного переноса электронов были изучены при помощи вейвлет-анализа. Релаксационная кинетика имеет S-образный характер зависимости от времени константы скорости возврата электрона от акцептора после выключения стимулирующего света. Релаксационные кривые RC являются нестационарными (зависят от времени). Рассмотрена двухуровневая модель переноса электронов. Центры реакции рассматриваются как динамические во времени и идентичные друг другу. Вейвлет-анализ кинетики релаксации позволяет предположить, что экспоненты релаксационных кривых не включаются одновременно, а появляются поочередно.

У даній роботі обговорюється кінетика переносу електронів у бактеріяльних реактивних центрах (РЦ). Аспекти релаксаційних процесів і фотоін-

дукованих структурних перетворень у молекулярному комплексі РЦ Rhodobacter sphaeroides як результат внутрішньомолекулярного переносу електронів було вивчено вейвлет-аналізою. Релаксаційна кінетика має *S*-подібний характер залежности від часу константи швидкости повернення електрона від акцептора після вимикання стимулювального світла. Релаксаційні криві РЦ є нестаціонарними (залежать від часу). Розглянуто дворівневий модель переносу електронів. Центри реакції розглянуто як динамічні у часі й ідентичні один до одного. Вейвлет-аналіза кінетики релаксації дозволяє припустити, що експоненти релаксаційних кривих не включаються одночасно, а з'являються по черзі.

1. INTRODUCTION

A photosynthetic reaction centre is a complex of three types of protein that is the site where molecular excitations originating from sunlight are transformed into a series of electron-transfer reactions. The reaction centre proteins bind functional co-factors, chromophores or pigments such as chlorophyll and pheophytin molecules. These ones absorb light, promoting an electron to a higher energy level. Free energy created is used to reduce a chain of electron acceptors, which have subsequently lowered redox-potentials, and is critical for the production of chemical energy during photosynthesis.

As known [1−5], the absorption of the light quantum in RC causes the photooxidation of the fundamental donor of the bacteriochlorophyll dimer (*P*) (Fig. 1) [6]. The excited electron through the series of intermediate transmitting agents gets on fundamental (Q_a) quinones acceptor (150 ps) and then on finite (Q_b) acceptor (10^{-4} s). Electron is carried
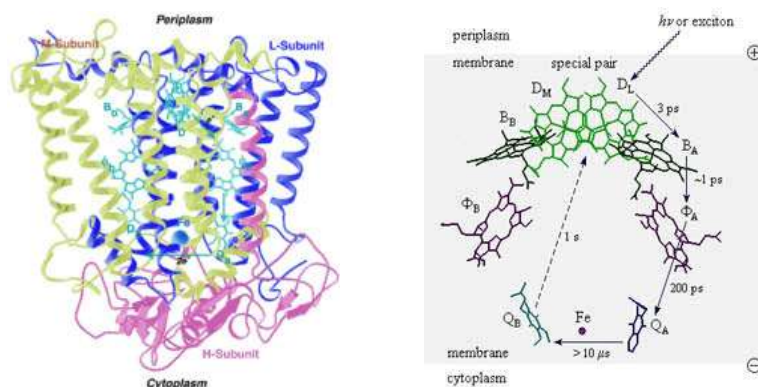

Fig. 1. The structure of RC and the scheme of electron phototransfer.

over at a distance equals to about 30 Å from P to Q_b. Determinative role in this process belongs to proteinaceous environment. Electron is in dynamic equilibrium at fixed illumination. Parameters of such equilibrium depend on intensity and exposure time. Absorbency of RC solution ($\lambda = 865$ nm) is diminished. After the light is turned off, the relaxation of RC to a dark state starts and sluggish return of an electron happens. Absorbency of RC solution ($\lambda = 865$ nm) is recovered. If the relaxation time of excited RC is bigger than time of light quantum inflow, we have build-up effect of structural changes in RC.

The main goal of our investigation was analysis of electron-transfer kinetics in bacterial RC by wavelet transformation.

2. MODEL APPROXIMATION

The described processes allow us to examine the RC system as a two-level one [7]. As consistent with this model, the RC are in the basic state (0) when an electron is localized on a donor P. During the absorption of light quantum, the RC passes to the excited state, and an electron is moved to acceptor Q_b—the state (1). Kinetics of this process is defined through rates of direct (k_{01}) and reverse (k_{10}) transition. Observation of these characteristics provides information concerning electron-conformational changes in RC. Transition rate of electron from donor to acceptor (k_{01}) is proportional to intensity of stimulating light I_0, so we can write that:

$$k_{01} = I_0 \alpha , \tag{1}$$

where α is time independent extinction coefficient.

Features of kinetics of RC are described by modelling of rate of reverse transition (k_{10}). It can be supposed that this rate depends on time. Kinetics of processes in RC affected by light can be described as:

$$\frac{dp(t)}{dt} = I_0 \alpha p(t) + k_{10}(t)(1 - p(t)) . \tag{2}$$

As the starting condition, we use the following one:

$$P(0) = 1 . \tag{3}$$

These conditions correspond to all electrons sit on donor before the light is turned on. Processes in RC complex when the light is turned off can be described by the equation similar to (2):

$$\frac{dq(t)}{dt} = -k_{10}^T(t)q(t) \ \text{ and } \ q(0) = q_0 , \tag{4}$$
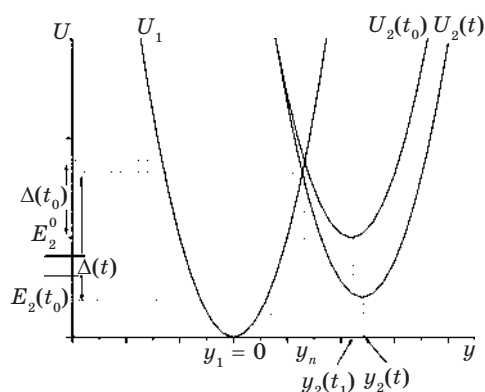
Fig. 2. The scheme of electron transitions in two-level system.

where parameter $k_{10}^T(t)$ defines the rate of transition from the acceptor (Q_b) to donor (P), when light is turned off; $q(t)$ is a probability of absence of an electron on the donor RC; q_0 describes absence of electron on donor at the moment of turning off lightening and depend on parameters of stimulating light and temperature of sample.

The relation similar to (4) can be written also for absorption $A(t)$ of solution of RC, which can be measured experimentally:

$$k_{10}^T(t) = \frac{\dfrac{dA(t)}{dt}}{\big(A(0) - A(t)\big)}.$$
(5)

Configuration of system is very important for macromolecules functioning. Evolution of this configuration can be retraced by kinetics of RC relaxation. Let us consider slow conformational movements emerged by redistribution of electron density. To explain the features of $k_{10}^T(t)$ behaviour, the particular model was suggested (Fig. 2). Electron can be on a donor (condition 1) or on an acceptor (condition 2). As affected by light, electron makes transition $1 \to 2$. Reversion of electron to the reference position is described by transition $2 \to 1$.

The electron in condition 1 is localized near a point y_1. Assuming that $y_1 = 0$, change in potential energy of electron by its deviation from equilibrium position can be described within the linear approximation by potential energy $U_1(y)$ in cusp form:

$$U_1(y) = \frac{a}{2}y^2,$$
(6)

where a is the parameter, which defines slope of potential sidetracks $U_1(y)$.

When electron makes transition to the condition 2, the centre of its equilibrium state shifts to the point y_2. In such case, surrounding of electron is changed, so its interaction has to change too. Potential energy of electron in condition 2 in linear approximation is as follows:

$$U_2(y) = \frac{b}{2}(y - y_2)^2 + E_2,\qquad(7)$$

where b is the parameter, which determines slope of potential sidetracks $U_2(y)$. E_2 determines minimum value of potential energy of electron in condition 2. It is supposed that location of electron neighbours in condition 2 is not rigid. Therefore, at the expense of interaction of electron with surroundings, polarization of the localization area is happen. This polarization has some time dependence.

E_2, b, and y_2 have some time dependence too. To explain the features of kinetics of $k_{10}^T(t)$, let us consider features of transition $2 \rightarrow 1$. Figure 2 shows the scheme of electron transitions in two-level system. The value of k_{10}^T was defined by features of barrier between 2 and 1 with correlation:

$$k_{10}^T(t) = \nu \exp\left(-\frac{\Delta(t)}{k_B T}\right).\qquad(8)$$

Here ν is frequency of electron coming up to barrier $\Delta(t)$, k_B is Boltzmann constant, T [K] is temperature of sample.

Position of function $U_2(y)$ depends on time. Figure 2 shows that potential barrier height Δ, which prevents transition $2 \rightarrow 1$, depends on time too, because it is determined by the cross point of plots $U_1(y)$ and $U_2(y)$. It is clear that value of barrier is decreased ($\Delta(t_1) > \Delta(t_2)$ when function U_2 is subsided). Therefore, we can make the conclusion that reversion of electron from condition 2 to 1 will be as easier as U_2 is subsided at the expense of polarization processes. Let us define dependence $\Delta(t)$ on value $E_2(t)$, which is minimally probable value of $U_2(y)$ at the moment t. Subsidence of $E_2(t)$ in relation to equilibrium dark state is $E_2^0 - E_2(t)$. Let us define cross point y_n for plots $U = U_1(y)$ and $U = U_2(y)$ from equation $U_1(y_n) = U_2(y_n)$. Using equation (7) and (8), we obtain such an expression for y_n:

$$y_n = \frac{-by_2(t) + \sqrt{2(a-b)E_2(t) + aby_2^{\,2}(t)}}{a - b}.\qquad(9)$$

In the case if $a = b$, this expression obtains such an easy form:

$$y_n(t) = \frac{ay_2^2(t) + 2E_2(t)}{2ay_2(t)}.\qquad(10)$$

Let us make assumption about probable $y_2(t)$ dependence. The shift

$\left(y_2^0 - y_2(t)\right)$ is proportional to the value of 'slump or subsidence' $E_2^0 - E_2(t)$, where y_2^0 is a grid point of the centre of level 2 in equilibrium dark stage. Therefore, we have correlation:

$$y_2^0 - y_2(t) = \alpha\left(E_2^0 - E_2(t)\right), \tag{11}$$

where α is a dimension coefficient of proportionality. Using (10) and (11), we can present the value of energy barrier $\Delta(t)$ as:

$$\Delta(t) = \frac{a}{8}\left[y_2{}^0 - \alpha\left(E_2{}^0 - E_2(t)\right)^2\right] + \frac{E_2{}^2(t)}{2a\left[y_2{}^0 - \alpha\left(E_2^0 - E_2(t)\right)^2\right]} - \frac{E_2(t)}{2}. \tag{12}$$

Last relation shows that the value of barrier for electron transition $2 \rightarrow 1$ is completely defined by kinetics of $E_2(t)$ and $y_2(t)$. The separate task is development of model for level 2 shifts. When electron is found on level 2 (with probability q), polarization of surroundings happens under electron electric field [8, 9]. Level 2 lowers. Let us suppose that the rate of electron potential energy decreasing is proportional to probability of electron being on level 2 (denote the proportionality coefficient μ). Electron leaves level 2 and relaxation of level to the initial value starts. Let us suppose that the rate of this process is proportional to the shift of initial level $\left(E_2^0 - E_2(t)\right)$. Characteristic time of relaxation τ does not depend on this shift. Therefore, the equation for level 2 dynamics is as follows:

$$\frac{dE_2(t)}{dt} = -\mu q(t) + \frac{E_2^0 - E_2(t)}{\tau}. \tag{13}$$

Starting condition for (13) is:

$$E_2(t = 0) = E_{2,0}, \tag{14}$$

where $E_{2,0}$ is the value of level 2 energy at the moment of turning off exited light.

Solution of (13), (14) is as follows:

$$E_2(t) = E_2{}^0 - \left(E_2{}^0 - E_{2,0}\right)\exp\left(-\frac{t}{\tau}\right) - \mu\int_0^t q(t^*)\exp\left(-\frac{t - t^*}{\tau}\right)dt^*. \tag{15}$$

The next condition has to be satisfied:

$$\left(E_2^0 - E_{2,0}\right) \geq 0. \tag{16}$$

Thus, the set of equations, which describes the process of electron return to the initial position on donor RC, is:

$$\frac{dq(t)}{dt} = -k_{10}^{T}(t)q(t), \quad k_{10}^{T}(t) = \nu \exp\left(-\frac{\Delta(t)}{k_B T}\right),$$

$$\Delta(t) = \frac{a}{8}\left[y_2^0 - \alpha\left(E_2^0 - E_2(t)\right)^2\right] + \frac{E_2^2(t)}{2a\left[y_2^0 - \alpha\left(E_2^0 - E_2(t)\right)^2\right]} - \frac{E_2(t)}{2}, \quad (17)$$

$$E_2(t) = E_2^0 - \left(E_2^0 - E_{2,0}\right)\exp\left(-\frac{t}{\tau}\right) - \mu\int_0^t q(t^*)\exp\left(-\frac{t-t^*}{\tau}\right)dt^*,$$

$$E_2(t=0) = E_{2,0}, \quad q(t=0) = q_0.$$

Rate constant of electron relaxation (donor recovery) considerably depends on probability of electron lack on donor. Therefore, the problem is self-consistent. Increase of deformation is proportional to the value of subsidence of level 2.

3. EXPERIMENTAL SETUP

The experimental investigations of changes in absorption coefficient of RC water solution in different modes of light were carried out. For experimental investigation of RC optical absorption kinetics, the hardware–software complex (Fig. 3) was developed. Hardware–software complex allows to measure kinetics of optical absorption of solutions in the range $0-1$ (± 0.0005) at the wavelength (λ) of 865 ± 10 nm.

Characteristics of this complex is low-intensity light (0.2 µW/sm^2, LED L53SF4BT), flashing with a frequency of 5 kHz and additional optical channel with $\lambda = 870\pm50$ nm and intensity up to 5 µW/sm^2 (LED L53SF6C).

Complex is constructed on the basis of IBM PC with conjugate plate in system unit of PC and digital and analogue data acquisition system. Complex consists of three major components. Optical scheme is placed in the first major component, signal-processing module—in the second, and digital-analogue conversion module—in the third one. Optical scheme module contains light-emitting diodes as testing and stimulating light sources, shaping channels of testing, stimulating light, and light, which was transmitted through solution. As a testing light source, one LED was used. The set of 10 LED with maximum power 50 mW was used as stimulation light. Stimulation light intensity can be regulated from 0 to 5 mW/sm^2 (step is 10 µW/sm^2). Optical scheme module provides forming of testing and stimulating light currents for appropriate LED in optical module, basic amplification of signal from measuring channel output in optical module up to ±10 V, digital division of amplified signals in measuring transmitted and testing light chan-

nels, taking the logarithm of amplification results, and testing light stabilization. Optical scheme module output is connected with input of digital-analogue converter module. Digital-analogue converter module consists of tree-channel analogue-to-digital converter with choice-storage device and one digital-to-analogue converter. Signal levels are from 0 to 10 V, conversion time is 200 μs, and resolution is 12 bit with parallel interface for connection with PC.

Hardware–software complex allows testing solutions in independent mode under the guidance of PC operator as consistent with defined program of investigation and provides digital indication of parameters and result of working under the management of 'Windows 98'.

In line with research technique of photostimulated electron transport in RC, the programs for hardware–software complex control were developed. These programs provide RC illumination mode with pulses which have different intensity up to 5 mW/sm^2 (step is 50 μW/sm^2) and different duration from 1 to 500 s. Measurement procedure is divided into 6 time intervals for the purpose of PC resources saving. On the first interval, 20 counts register initial value of RC solution absorption. During front acting or pulse trail of stimulation light (the second and the fourth intervals) 5 s, the sampling increment was constant (0.01 s). During the third interval (RC illumination) and the fifth interval (RC relaxation), the sampling increment and number of steps were determined programmatically according to experimental conditions. During the sixth interval (RC relaxation), the sampling increment in time was 1
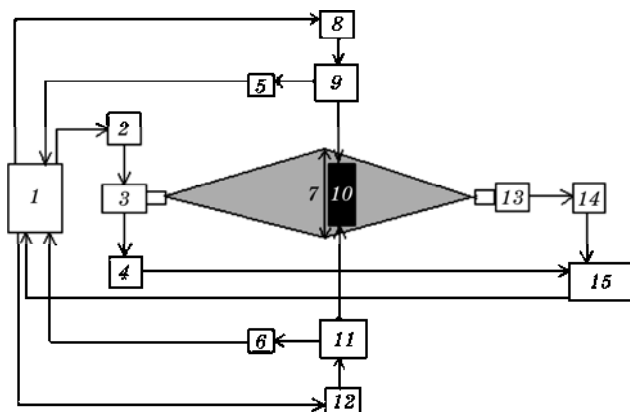

Fig. 3. Block diagram of arrangement: *1*—PC; *2*—testing light-shaping channel; *3*—testing light-emitting diode **(LED)** system; *4*—measuring line of testing light intensity; *5*, *6*—measuring line of stimulating light intensity; *7*—focusing lens; *8*, *12*—stimulating light-shaping channel; *9*, *11*—light-emitting diode system of stimulating light; *10*—cell with solution of RC; *13*—photodetector; *14*—preamplifier; *15*—signal processing module and digital-analogue converter module.
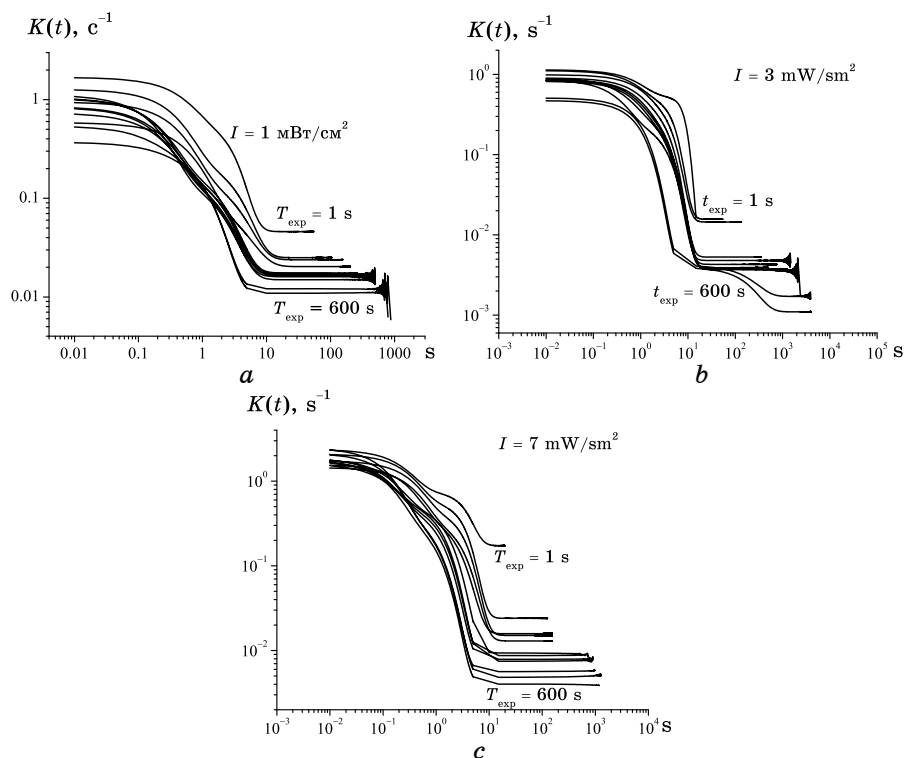
Fig. 4. Dependence of change of absorption in water solution of RC after stimulating light was turned off (after turning off of stimulating light) ($t = 0$ sec) for different values of exposure time (1, 5, 10, 20, 30, 40, 50, 60, 90, 120, 300, 600 sec), $I_0 = 1, 3, 7$ mW/sm^2.

s. Number of steps was defined by time for RC solution absorption recovery to initial value. For this purpose, comparison of current and initial (measured on the first interval) absorption value was carried out. As soon as RC solution absorption value (after 20 counting) became equal to initial RC solution absorption value, measurement was stopped. Such measurement procedure reduces influence of human factor and provides replicable experimental results.

Figure 4 shows the observed resulted speed of change of absorption $(K(t))$ after the light was turned off. Light intensity was 1, 3, 7 mW/sm^2.

The relaxation rate of structural changes in RC after the light was turned off had S-shaped mode. The changes vary in a range of times from 0.2–0.4 sec (initial field) up to 6–10 sec (finite field) depending on conditions of experiment. Rates of relaxation of RC on initial and finite periods differ by tens time.

Thus, structural changes of RC occur at the expense of electrostatic field, which emerges as the result of extension of gap be-

tween Q_a and Q_b. Transfer process is cyclic. As longer electron stays on acceptor so long, the distortions appear:

$$K(t) = \left| \frac{A'(t)}{A(t)} \right| = k'(t)t + k(t), \tag{18}$$

where $A(t) = v \exp\left(-k(t)t\right)$ is absorption coefficient. For different k, we have different degrees of structural changes.

The next step of our investigation was wavelet analysis of the experimental diagrams. Application of wavelet analysis is predetermined by the lacks of fitting and Fourier analysis. When we use fitting with exponential function, the same experimental curves can be described by different sets of parameters k and v. It causes ambiguity of expansion. Therefore, the problem solution is incorrect. Relaxation curves are nonstationary (time-dependent). Therefore, time localization is necessary. Fourier analysis does not allow getting time-and-frequency representation of a signal. Wavelet analysis allows getting some features of the S-shaped curves such as critical points or points of frequency changing.

4. WAVELET ANALYSIS

Wavelets are mathematical functions that cut up data into different frequency components, and then study each component with a resolution matched to its scale. They have advantages over traditional Fourier methods in analyzing physical situations where the signal contains discontinuities and sharp spikes.

The main disadvantage of Fourier expansion is that it has only frequency resolution and no time resolution. That means that although we might be able to determine all the frequencies present in a signal, we do not know when they are present. The idea behind these time-frequency joint representations is to cut the signal of interest into several parts and then analyze the parts separately. The problem here is that cutting the signal corresponds to a convolution between the signal and the cutting window. The underlying principle of the phenomena just described is connected with Heisenberg's uncertainty principle, which, in signal processing terms, states that it is impossible to know the exact frequency and the exact time of occurrence of this frequency in a signal. In other words, a signal can simply not be represented as a point in the time-frequency space. The uncertainty principle shows that it is very important how one cuts the signal.

The wavelet transform or wavelet analysis is probably the most recent solution to overcome the shortcomings of Fourier transform. In wavelet analysis, the use of a fully scalable modulated window solves the signal-cutting problem. The window is shifted along the signal and

the spectrum is calculated for every position. Then this process is repeated many times with a slightly shorter (or longer) window for every new cycle. At the end, the result will be a collection of time-frequency representations of the signal, all with different resolutions. Because of this collection of representations, we can speak about a multiresolution analysis. In the case of wavelets, we normally do not speak about time-frequency representations, but about time-scale representations, scale being in a way the opposite of frequency, because the term frequency is reserved for the Fourier transform.

Formally, the continuous wavelet transform (CWT) can be written as:

$$\gamma(a, b) = \int f(t)\Psi_{a,b}^{*}(t)dt, \tag{19}$$

where * denotes complex conjugation. This equation shows how a function $f(t)$ is decomposed into a set of basis functions $\Psi_{a,b}(t)$, called the wavelets. The variables a and b, scale and translation, are new dimensions after the wavelet transform. The inverse wavelet transform is

$$f(t) = \iint \gamma(a, b)\Psi_{a,b}(t)dadb. \tag{20}$$

The wavelets are generated from a single basic wavelet $\psi(t)$, the so-called mother wavelet, by scaling and translation:

$$\Psi_{a,b}(t) = \frac{1}{\sqrt{a}} \Psi\left(\frac{t - b}{a}\right). \tag{21}$$

In Eq. (21), a is the scale factor, b is the translation factor, and the factor $a^{-1/2}$ serves for energy normalization across the different scales [10].

The wavelet basis functions are not specified. This is a difference between the wavelet transform and Fourier transform, or other transforms. The theory of wavelet transforms deals with the general properties of the wavelets and wavelet transforms only. It defines a framework within one can design wavelets to taste and wishes. For example, Figure 5 shows us wavelets Mhat (Mexican hat) and Wave:

$$\psi_{Mhat}\left(t, a, b\right) = \frac{1,031}{\sqrt{2}} \left\{\exp\left[-\left(\frac{t - b}{a}\right)^{2}\right] - 2\left(\frac{t - b}{a}\right)^{2} \exp\left[-\left(\frac{t - b}{a}\right)^{2}\right]\right\}, \tag{22}$$

$$\psi_{wave}\left(t, a, b\right) = \frac{-1,786}{\sqrt{2}} \frac{t - b}{a} \exp\left[-\left(\frac{t - b}{a}\right)^{2}\right]. \tag{23}$$

Let us consider wavelet properties. The most important properties of wavelets are the admissibility and the regularity conditions and these are the properties, which gave wavelets their name. It can be shown that square integrable functions $\psi(t)$ satisfying the admissibility condition,
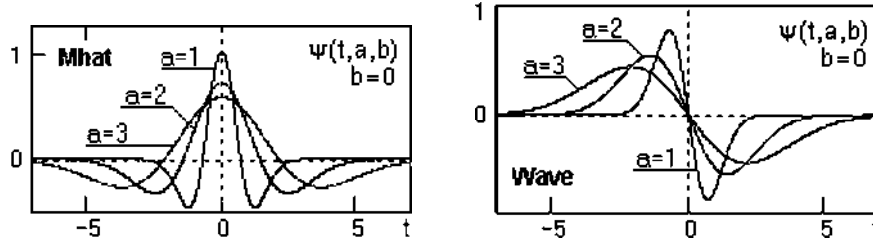
Fig. 5. Wavelets Mhat and Wave.

$$\int \frac{\left| \Psi \left(\omega \right) \right|^2}{\left| \omega \right|} d\omega < +\infty \,, \tag{24}$$

can be used to first analyze and then reconstruct a signal without loss of information. In Eq. (24), $\Psi \left(\omega \right)$ stands for the Fourier transform of $\psi(t)$. The admissibility condition implies that Fourier transform of $\psi(t)$ vanishes at the zero frequency, *i.e.*

$$\left| \Psi \left(\omega \right) \right|^2 \big|_{\omega=0} = 0 \,. \tag{25}$$

This means that wavelets must have a band-pass like spectrum.

A zero at the zero frequency also means that the average value of the wavelet in the time domain must be zero,

$$\int \psi(t) dt = 0 \,; \tag{26}$$

Therefore, it must be oscillatory. In other words, $\psi(t)$ must be a wave.

The wavelet transform of a one-dimensional function is two-dimensional; the wavelet transform of a two-dimensional function is four-dimensional. The time-bandwidth product of the wavelet transform is the square of the input signal and, for most practical applications, this is not a desirable property. Therefore, one imposes some additional conditions on the wavelet functions in order to make the wavelet transform decrease quickly with decreasing scale a. These are the regularity conditions and they state that the wavelet function should have some smoothness and concentration in both time and frequency domains. Regularity is a quite complex concept and we will try to explain it using the concept of vanishing moments.

Wavelet analysis makes it possible to get not only frequency response but also information about local coordinates for definite frequency components or coordinates of rapid frequency components changes.

Spectrum of one-dimension signal is the surface in tree-dimension space. Different ways of spectrum visualization exist. The most com-
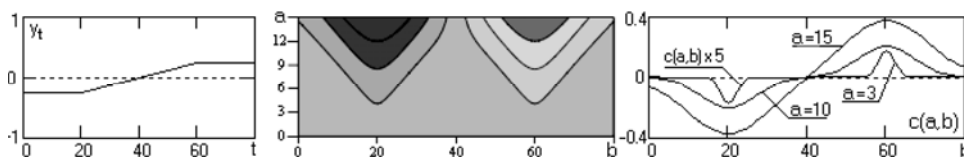
Fig. 6. Signal, wavelet spectrum (Mhat) and scale section for it.

mon method is the plane *ab* projection with isolines. It makes possible to trace coefficient changes for different time scale and find local extremes of this surface, so-called skeleton. Figure 6 shows the example of wavelet spectrum of the simple signal **[11, 12]**.

The choice of certain wavelet kind depends on signal appearance and the task of analysis. This choice is subjective but can bring new possibilities for the analysis. Different wavelet testing is necessary.

5. RESULTS AND DISCUSSION

Three types of wavelet were tested: Wave, Mhat and complex wavelet Morlet. By the analysis of check curves, it is possible to define to what features of curves each of considered wavelets is sensible.

For investigation of experimental curves of RC, complex relaxation wavelet of Morlet is the most suitable.

$$\psi_{Morlet}(t, a, b) = \frac{1}{\pi\sqrt{a}}\left[\exp\left(-i\varepsilon\left(\frac{t-b}{a}\right)\right) - \exp\left(-\frac{\varepsilon^2}{2}\right)\exp\left(-\left(\frac{t-b}{a}\right)^2\varepsilon\right)\right]. (27)$$

Figure 7 shows decrements $\left(FTest_i\left(t_i\right)\right)$ and wavelet spectra $\left(M\arg_b(dTb)\right)$ of check curves.

So, if the damping decrement (damping constant) of curve does not change with time (test curves 1−3), then wavelet spectrum of such curve does not have pronounced features (except boundary conditions).

In case of hyperbolic dependence (test curve 4), we have dome-shaped spectrum. This case needs further exploration. Test curve 5 has several cascades, which show how the curves decrements change. Wavelet spectra have pronounced peaks in this place.

Several series of experimental curves for different ranges of lighting (intensity of light 100, 300, 700 units or 1, 3, 7 mW/sm^2) and for different exposure time (1, 5, 10, 20, 30, 40, 50, 60, 90, 120, 300, 600 seconds) were analyzed.

Figure 8 shows wavelet spectra of relaxation curves. Wavelet parameter $a = 3$. Wavelet spectra of relaxation curves have pronounced features, so analysis of experimental curves shows certain $K(t)$ time dependence.
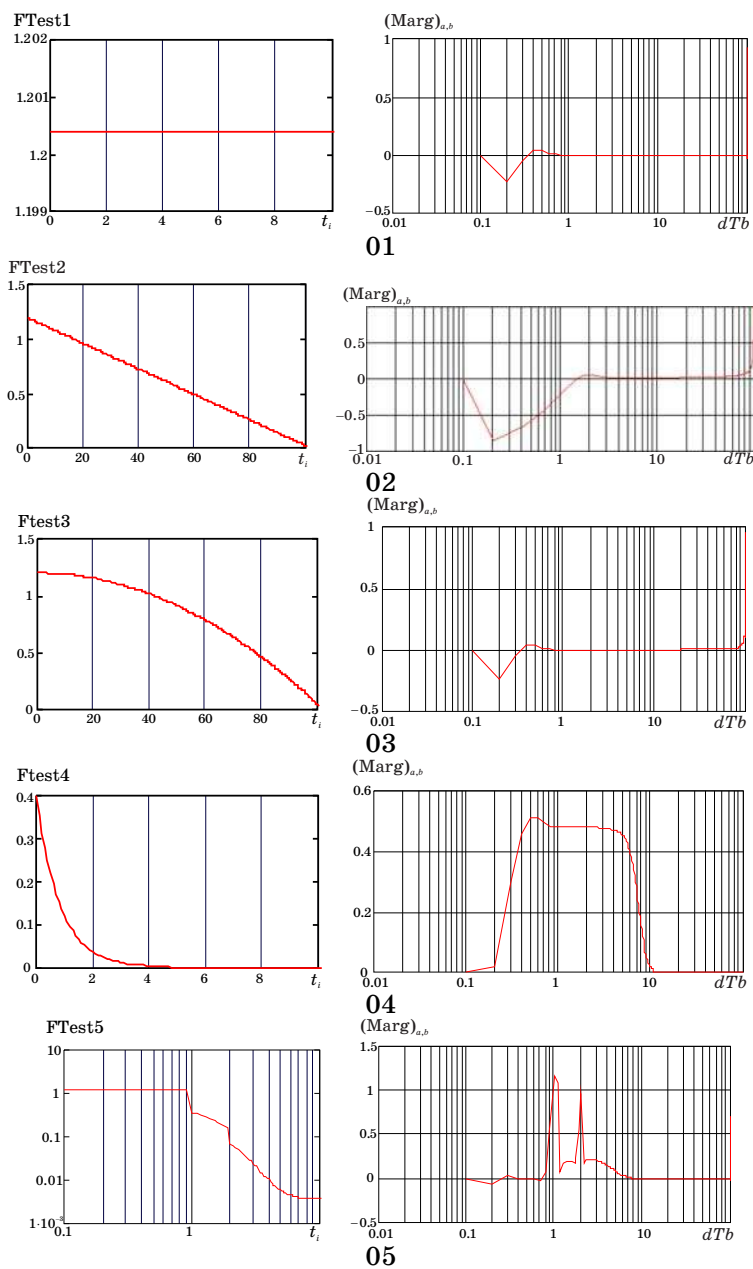
Fig. 7. Test curves and their wavelet spectra (Morlet).

Let us analyze appearance of test wavelet spectra and draw the analogy with spectra of experimental relaxation curves. The first peak of relaxation curves wavelet spectra can be correlated with peak of spec-
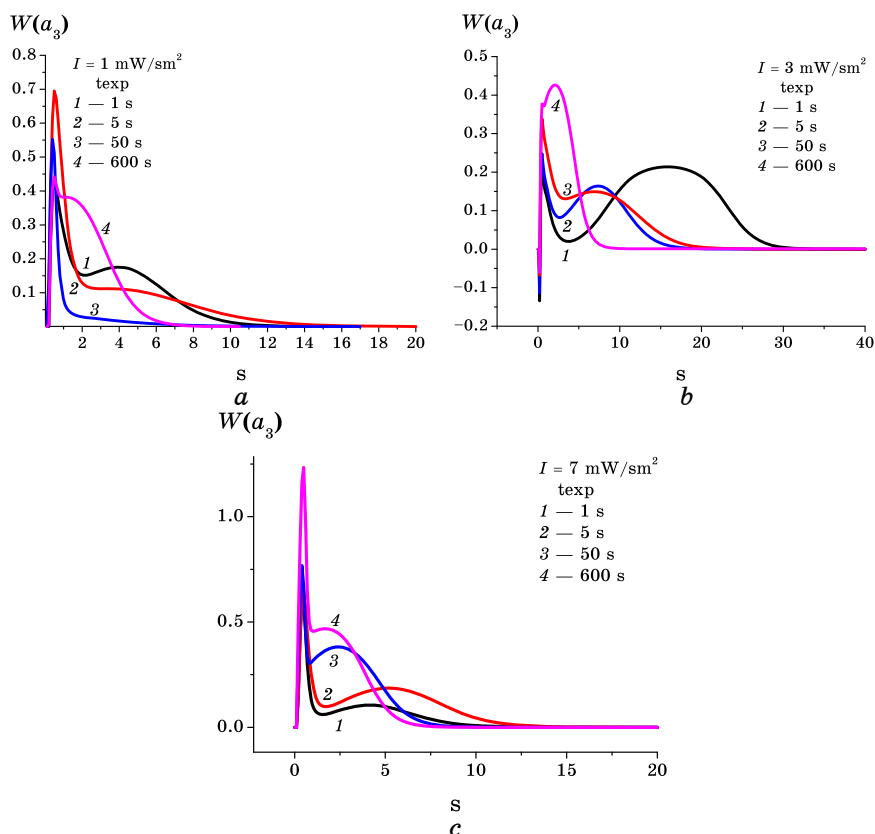
Fig. 8. Wavelet spectra of relaxation curves ($a = 3$).

tra of test curve 5. Let us suppose that at the beginning of relaxation process a fast channel of relaxation exists. The first peak is the end of the fast channel operation. Then, slow channel switches on. Second peaks are not expressed, diffused and dome-shaped similarly to spectrum of test curve 4.

This feature can be explained through the sets of exponent shifts or relaxation curves on this interval, which have the same functional dependence as test curve 4.

For the different values of intensity and exposure time, the second peaks have different appearance. The first peaks are the same for all experimental curves. Qualitative differences of wavelet spectra dependent on exposure time mean qualitative changes of RC stage.

6. SUMMARY

Relaxation rate of RC structural changes after 10 seconds changes

negligible in time. Relaxation rate depends on intensity of stimulating light and exposure time. S-shaped mode of relaxation rate does not depend on intensity of stimulating light and exposure time.

The wavelet analysis shows us experimental relaxation curves features, which depend on intensity of stimulating light and exposure time. These features are changes of curves spectral composition in time. Thus, we can suppose that relaxation exponents do not operate simultaneously but switch on alternatively (in turn). Rapid and slow channels of relaxation exist. It means that RC is dynamic in time and all RC are the same.

REFERENCES

1.   A. B. Rubin, *Biophysics* (Moscow: Moscow University: 2000) (in Russian).
2.   V. A. Shuvalov and V. A. Klimov, *Biophysics*, **32**, No. 5: 814 (1987) (in Russian).
3.   J. M. Olson and J. P. Thornber, *Membrane Proteins in Energy Transduction* (Ed. R. A. Capaldi) (New York: 1979).
4.   T. Gensch, C. Viappiani, and S. E. Braslavsky, *Journal of the American Chemical Society*, **121**: 10573 (1999).
5.   T. V. Komarevska, S. I. Kshniakina, and M. A. Zabolotny, *Naukovi Zapysky of NaUKMA*, **61**: 54 (2007) (in Ukrainian).
6.   G. Triskunas and L. Valkunas, *Physical Phenomena in Photosynthesis* (Vilnius: Znanie: 1986) (in Russian).
7.   Y. M. Barabash, M. A. Zabolotny, N. I. Sokolov, and V. N. Kharkyanen, *Biophysics*, **6**: 152 (2002) (in Russian).
8   K. V. Shaitan, *Soros Educational Journal*, **3**: 55 (1999) (in Russian).
9.   K. V. Shaitan, *Soros Educational Journal*, **5**: 5 (1999) (in Russian).
10.   C. K. Chui, *Introduction to Wavelets* (Moscow: Mir: 2001) (in Russian).
11.   H.-G. Stark, *Wavelets and Signal Processing* (Moscow: Tekhnosfera: 2007) (in Russian).
12.   S. Malat, *Wavelet Tour of Signal Processing* (Moscow: Mir: 2005).